

Dust Aerosol Important for Snowball Earth Deglaciation

DORIAN S. ABBOT

Department of Geophysical Sciences, University of Chicago, Chicago, Illinois

ITAY HALEVY

Department of Earth and Planetary Sciences, Harvard University, Cambridge, Massachusetts

(Manuscript received 11 August 2009, in final form 28 December 2009)

ABSTRACT

Most previous global climate model simulations could only produce the termination of Snowball Earth episodes at CO₂ partial pressures of several tenths of a bar, which is roughly an order of magnitude higher than recent estimates of CO₂ levels during and shortly after Snowball events. These simulations have neglected the impact of dust aerosols on radiative transfer, which is an assumption of potentially grave importance. In this paper it is argued, using the Dust Entrainment and Deposition (DEAD) box model driven by GCM results, that atmospheric dust aerosol concentrations may have been one to two orders of magnitude higher during a Snowball Earth event than today. It is furthermore asserted on the basis of calculations using NCAR's Single Column Atmospheric Model (SCAM)—a radiative-convective model with sophisticated aerosol, cloud, and radiative parameterizations—that when the surface albedo is high, such increases in dust aerosol loading can produce several times more surface warming than an increase in the partial pressure of CO₂ from 10⁻⁴ to 10⁻¹ bar. Therefore the conclusion is reached that including dust aerosols in simulations may reconcile the CO₂ levels required for Snowball termination in climate models with observations.

1. Introduction

There is good evidence that at least twice during the Neoproterozoic, about 710 million years ago and about 635 million years ago, there were glaciers at sea level in the tropics (Kirschvink 1992; Evans 2000; Trindade and Macouin 2007). According to the Snowball Earth hypothesis these glaciations occurred contemporaneously around the planet, the oceans were entirely covered with sea ice for millions of years, and the climate recovered only when volcanic outgassing slowly brought the partial pressure of CO₂ ($p\text{CO}_2$) to such extremely high values that tropical surface temperatures exceeded the freezing point of water despite the high reflectivity of the ice-covered surface (Kirschvink 1992; Hoffman et al. 1998).

There are several lines of evidence for high $p\text{CO}_2$ at the end of long panglacial episodes. First, many of the glacial sediments are overlain by carbonates in sedimentary

successions that are otherwise siliciclastic (Hoffman and Li 2009). These carbonates are interpreted to have formed as the massive store of atmospheric CO₂ precipitated with weathering-derived calcium when the ice finally melted and the ocean was exposed to the atmosphere. The carbonates are in some cases hundreds of meters thick (Hoffman and Li 2009), suggesting that millions of years of subsidence created the space required for their accommodation. Furthermore, interpretations of the carbon isotopic composition recorded in the carbonates suggest high $p\text{CO}_2$ (Higgins and Schrag 2003).

Another piece of evidence in support of the Snowball Earth hypothesis is the iron and iron-manganese deposits found in glacial sediments (Hoffman and Li 2009), which may indicate anoxic conditions that would result if an ice-covered ocean were isolated from the atmosphere for a prolonged period. Even so, the Snowball Earth hypothesis is still in dispute (Kerr 2000; Hyde et al. 2000; Allen and Etienne 2008; Peltier et al. 2007; Hoffman et al. 2008; Peltier and Liu 2008).

Recent measurements of oxygen isotopic anomalies in sulfate minerals indicate that $p\text{CO}_2$ during and just after the Marinoan glaciation (~635 million yr ago)

Corresponding author address: Dorian S. Abbot, Department of Geophysical Sciences, University of Chicago, 5734 South Ellis Avenue, Chicago, IL 60637.
E-mail: abbot@uchicago.edu

reached 0.01–0.08 bar (Bao et al. 2008, 2009), although these values do not necessarily represent the peak $p\text{CO}_2$. This presents a problem, because with Neoproterozoic solar luminosity ($\sim 94\%$ present) and the high reflectivity (albedo) of ice and snow, most climate simulations do not reach the surface temperatures required for deglaciation until $p\text{CO}_2$ is increased to a few tenths of a bar (Pierrehumbert 2004, 2005; Le Hir et al. 2007; Abbot and Pierrehumbert 2010). Caldeira and Kasting (1992) were able to deglaciate a Snowball using a one-dimensional energy balance model with annual mean present-day solar luminosity, no atmospheric or ice dynamics, and $p\text{CO}_2$ of 0.12 bars. The global average temperature at which deglaciation occurred, however, was assumed to be 263 K, which may be unrealistically low for low-latitude ice. When the appropriate luminosity is accounted for, such models only reach 273 K for $p\text{CO}_2 > \sim 0.3$ bars (Pierrehumbert 2005), and higher values of $p\text{CO}_2$ might be required if atmospheric and ice dynamics were accounted for. Under a limited subset of conditions, a coupled energy balance–sea ice model has produced thin sea ice in the tropics, allowing deglaciation at $p\text{CO}_2 = \sim 0.01$ bar (Pollard and Kasting 2005), but it is uncertain whether the parameter regime in which this solution exists is realistic (Warren and Brandt 2006; Pollard and Kasting 2006).

Common to all of the paleoclimate studies mentioned above are uncertainties in three important properties: the surface albedo during a Snowball, cloud feedbacks, and absorption by high abundances of CO_2 . The albedo of clean snow and ice varies between values of 0.5 and 0.9 (Warren et al. 2002), and most climate studies adopt a value between 0.6 and 0.7. However, dirty snow and ice are much less reflective and so the deglaciation of a dirty Snowball requires correspondingly lower levels of atmospheric CO_2 (Abbot and Pierrehumbert 2010). Additionally, the cloud processes that would operate during Snowball events are not well understood and cloud feedbacks could cause strong warming and help to promote deglaciation (Le Hir et al. 2007; Abbot and Pierrehumbert 2010). Finally, the radiative forcing of ~ 0.1 bar of CO_2 is also uncertain because of inadequate formulation of absorption in the CO_2 window regions (Halevy et al. 2009). The difference in radiative forcing between existing parameterizations of CO_2 absorption at abundances relevant to deglaciation of a Snowball is $\sim 8 \text{ W m}^{-2}$, equivalent to an uncertainty in surface temperature of at least $\sim 4 \text{ K}$. Even with these uncertainties, it remains unclear that the CO_2 levels required for deglaciation in the climate models were ever reached. An important omission from previous studies is the effect of dust aerosols on the planetary energy budget. Here we report the results of radiative–convective calculations, which

show that dust aerosol concentrations appropriate for a Snowball allow deglaciation at $p\text{CO}_2$ as low as several hundredths of a bar, consistent with the paleo- $p\text{CO}_2$ proxy estimates.

There is good reason to believe that during Snowball episodes increased production and decreased removal rates would have combined to produce dust aerosol concentrations significantly higher than modern. Wet deposition or rainout, the main process by which dust is removed from the current atmosphere (Harrison et al. 2001), would have been significantly inhibited by the relatively inactive hydrological cycle during a Snowball. Furthermore, it is likely that large continental regions remained unglaciated because of low snowfall (Kirschvink 1992), as Siberia did during the Last Glacial Maximum. Climate models produce varying levels of perennial snow cover in continental interiors during Snowball episodes (Donnadieu et al. 2003; Pierrehumbert 2005) but may not be reliable for predicting unglaciated continental regions, since most climate models predict glaciers in Siberia during the Last Glacial Maximum (Kronner et al. 2006). Any exposed continental regions, even if small, would have been nonvegetated (land plants did not evolve until the Silurian, about 425 million years ago), extremely dry, and racked by extreme diurnal and annual temperature variations during a Snowball, all of which would tend to increase cryogenic weathering (Konishchev 1982) and thus dust production. Support for this idea comes from ice core and marine records, which indicate that during the more recent and less extensive glaciations of the Pleistocene (1.8 million years–10 000 years ago) dust aerosol concentrations were 2–20 times present-day values (Harrison et al. 2001). Further support comes from experimental and observational studies of the effect of temperature swings on physical weathering rates, which show that a combination of thermal stress, freeze–thaw, and wetting–drying cycles under arid conditions result in enhanced rates of physical weathering (Hall 1998; Elliott 2008).

Soil dust aerosols both reflect and absorb solar radiation. When the surface albedo is relatively low, as is the case for present-day oceans, dust tends to cool the surface because it scatters radiation that would otherwise reach the surface and be mostly absorbed. When the surface is highly reflective, as regions of clean ice and snow would be during a Snowball, scattering by dust aerosols is less important because most of the radiation is reflected from the planet's surface anyway. Under such conditions the absorption by dust aerosols of downwelling solar radiation and upwelling shortwave radiation reflected by the surface can lead to significant warming. Moreover, the relative abundance of aerosol types during Snowball episodes would lead to even stronger positive

forcing; sea salt and ammonium-sulfate aerosols, which are highly reflective and absorb shortwave radiation only very weakly, would have been all but absent if the oceans from which they originate were ice covered. Finally, mineral dust aerosols also absorb longwave radiation, which would lead to additional warming.

Observational support for the claim that soil dust during a Snowball should warm the surface comes from studies of the radiative effect of Saharan dust over variably reflective surfaces. Over the Atlantic Ocean, which has an albedo of less than 0.1, Saharan soil dust aerosols provide a calculated net negative forcing of 36–60 W m^{-2} , depending on the optical properties of the dust aerosols used (Weaver et al. 2002). The net forcing by soil dust with the same optical properties over the desert itself, which has an albedo as high as ~ 0.4 (Tetzlaff 1983), is positive and has a magnitude between 13 and 59 W m^{-2} (Weaver et al. 2002). In general, the net top-of-atmosphere forcing by soil dust is observed to increase monotonically with increasing surface albedo, becoming positive for values of the albedo slightly higher than 0.1 (Bierwirth et al. 2009).

Soil dust was probably more abundant during Snowball events and provided net positive radiative forcing over the highly reflective surface. It thus seems likely that soil dust played an important role in the climatic recovery from Snowball episodes. Below we present calculations that support this idea.

2. Methods

The large uncertainties in greenhouse gas concentrations, aerosol concentrations, and surface albedo during a Snowball necessitate the use of relatively simple models to investigate the system. Such models allow the exploration of large regions of parameter space without prohibitive numerical cost so that interesting behavior may be discovered. Furthermore, making assumptions about three-dimensional distributions of dust aerosols during a Snowball for use in GCMs seems unwarranted when fundamental properties such as the total magnitude of dust aerosol forcing, the surface albedo, and the oceanic heat transport, among others, are unknown. In this vein we use a dust box model to estimate the increase in dust aerosol concentration that could be expected during a Snowball event (section 2a), and we determine the warming this increase in dust would produce using a radiative–convective model that has only one spatial dimension (vertical) but contains sophisticated longwave and shortwave radiation, aerosol, and cloud schemes (section 2b). We perform a large number of simulations over a range of surface albedos, soil dust aerosol concentrations, and $p\text{CO}_2$ ranging from 10^{-4} to 10^{-1} bar.

a. Order of magnitude dust modeling

In steady state, the total dust aerosol loading in the atmosphere can be written as the product of the surface area of the dust source regions, the dust surface flux, and the dust lifetime. The factor by which the dust loading increases from modern to Snowball conditions (“dust factor”) D can be expressed as the product of the factors by which dust flux from the surface to the atmosphere S , source area of dust-producing regions A , and dust lifetime L increase:

$$D = S \times A \times L. \quad (1)$$

We use relatively simple methods to make scaling estimates for S , A , and L , described below. An alternative method for determining the scale of the atmospheric dust loading would be to use a sophisticated global dust model, such as that used by Mahowald et al. (2006a). Using such a model to simulate Snowball conditions, however, would involve choosing values for a large number of uncertain parameters to which the results would be extremely sensitive. For example, Mahowald et al. (2006a) find that even when simulating the relatively well-constrained Last Glacial Maximum, the dust flux estimates that a sophisticated global dust model produces in large regions of the Northern Hemisphere can differ by 1–3 orders of magnitude as a result of tuning a few uncertain source parameters. Therefore we do not believe that such a model would yield a more accurate order of magnitude for Neoproterozoic dust aerosol loading than our methodology.

To determine the increase in S that can be expected during a Snowball event, we use the Dust Entrainment and Deposition (DEAD) box model (Zender et al. 2003), which includes detailed parameterizations for dust production and mobilization and is the fundamental dust model coupled by Mahowald et al. (2006a) to a GCM. To simulate modern dust flux from source regions, we set the vegetation area fraction to 0.20, the volumetric water content to $0.05 \text{ m}^3 \text{ m}^{-3}$, and the surface temperature to 20°C . It is difficult to defend any particular choice of such parameters for scaling estimates such as those we make, but these choices may be considered reasonable insofar as they yield a total dust burden of 39 Tg, which is similar to the value of 22–31 Tg that Mahowald et al. (2006a) calculate for the modern climate. To simulate dust flux in cold, dry, and nonvegetated Snowball conditions, we set the vegetation area fraction and the volumetric water content to zero and the surface temperature to -10°C . The dust source flux produced by the DEAD model in both cases is shown in Fig. 1.

We then determine a characteristic dust flux scale for a particular climate F^* by calculating the mean

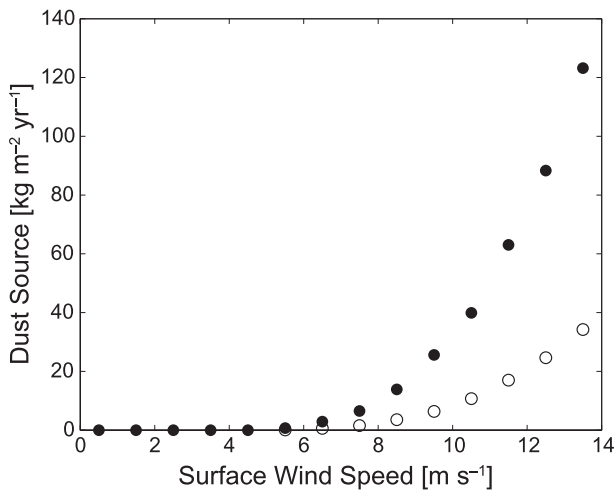


FIG. 1. Dust flux calculated with the DEAD box model as a function of surface wind speed for Snowball (filled circles) and modern (open circles) conditions. See text for details.

DEAD-produced dust flux $F(u)$ (Fig. 1) weighted by the probability distribution function (PDF) of surface wind speed over land produced in simulations performed using the National Center for Atmospheric Research (NCAR) Community Atmosphere Model (CAM) GCM run at T42 horizontal resolution with 26 vertical levels,

$$F^* = \int_0^{\infty} P(u)F(u) du, \quad (2)$$

where $P(u)$ is the probability of wind speed u (Fig. 3).

For the modern atmosphere we use a CAM simulation with 280 ppm CO_2 , modern continental and vegetative boundary conditions, and a slab ocean with specified modern ocean heat transport (Abbot et al. 2009). We refer to this simulation as “Modern” below. For the Snowball atmosphere we use two simulations performed by Abbot and Pierrehumbert (2010) with a tropical supercontinent similar to that of Pierrehumbert (2005) and 100 ppm CO_2 . These simulations are identical except that in one case CAM’s sea ice parameterization is used for the ice surrounding the continent (“Snowball 1”) and in the other CAM’s glacial ice parameterization is used (“Snowball 2”). In CAM, sea ice and glacial ice have fairly different surface properties, with the most important difference being that glacial ice is much more reflective. As a result of these differences, in simulations where the parameterization of glacial ice is used (Snowball 2) the typical climatic characteristics of a Snowball (i.e., low temperature, low precipitation, high wind speeds, etc.) tend to be more extreme. For a more detailed description of the CAM simulations see Abbot and Pierrehumbert (2010). Since little is known about

topography during the Neoproterozoic, the continents in the Snowball simulations are chosen to be flat. As wind speed generally increases with altitude, we only count grid points lower than 500 m when generating the surface wind PDF for the Modern simulation in order to facilitate a fair surface wind comparison between Snowball and modern conditions.

In estimating the change in A we consider the factors affecting the suitability of land regions for production of dust. The modern surface area of dust-producing regions is most strongly affected by the related conditions of vegetative cover and soil moisture. Using the methodology of Mahowald et al. (2006a) and the satellite-based vegetation maps of Bonan et al. (2002), we calculate that strong dust source regions represent 12.5% of the land area on modern earth. During a Snowball, however, all unglaciated continental regions would be nonvegetated and dry, so the fraction of glaciated land f_g is the appropriate property to consider when estimating the surface area of dust-producing regions. Despite the difficulty in obtaining a reliable estimate of f_g (discussed in section 1), we use the same CAM runs described above to estimate this property and from this we calculate the increase in dust source surface area as

$$A = \frac{1 - f_g}{0.125}. \quad (3)$$

In this treatment we neglect two factors. Since only low-lying regions serve as the most efficient centers of dust production in the modern (Zender et al. 2003), the fraction of unglaciated land may represent an overestimate of the area of dust-producing regions. On the other hand, dust accumulation on the surface of glaciated regions where sublimation exceeds precipitation of new snow (Abbot and Pierrehumbert 2010) could lead to the formation of new dust-producing regions. In neglecting these regions, which may have been expansive, we may underestimate the area of dust production. Although an underlying assumption of our treatment is that these two factors nearly cancel each other out, we note the large uncertainty in the relative importance of these factors.

Finally, we use the findings of previous studies to estimate L rather than estimating it directly. Dust is removed from the modern atmosphere by both wet and dry deposition. As global mean precipitation scales with global mean energy absorbed at the surface (Pierrehumbert 2002; Held and Soden 2006), the relatively high albedo during a Snowball should lead to greatly reduced global mean precipitation. Wet deposition of dust, however, does not necessarily scale directly with the magnitude of global mean precipitation. For example, model calculations

suggest that smaller, but more frequent, precipitation events during the Last Glacial Maximum kept the wet deposition rate roughly the same as modern (Mahowald et al. 2006a). Additionally, wet deposition of dust can function below the freezing point of water since snow is capable of scavenging dust. Therefore, even though calculations showing that the global mean precipitation was probably an order of magnitude lower than present during Snowball events (Pierrehumbert 2004, 2005; Abbot and Pierrehumbert 2010) suggest that the wet deposition rates were lower than modern, it remains unclear what these rates would be.

This said, it may be argued that the lifetime of the radiatively important dust fraction was greatly increased. Model calculations indicate that the size-averaged dust lifetime in the modern atmosphere of 2.7 days is produced by a wet deposition lifetime of 8.0 days and a dry deposition lifetime of 4.0 days (Mahowald et al. 2006a). However, the small dust particles that interact most strongly with radiation have much longer lifetimes to dry deposition (Mahowald et al. 2006a), leading to total (wet + dry) lifetimes that are governed mostly by their wet deposition lifetime. For example, dust particles of diameter 0.1–1 and 1–2.5 μm have dry deposition lifetimes ~ 35 and ~ 10 times longer than their total lifetimes, respectively. It is enough that wet deposition is halved, not decreased by an order of magnitude like the global mean precipitation, for the lifetime of the radiatively important dust fraction to essentially double. This means that an increase in the size-averaged lifetime of dust of $\sim 50\%$ ($L \sim 1.5$), which would be calculated in the complete absence of wet deposition, may in fact represent a conservatively low estimate for L . We adopt this value for L , noting again the uncertainty associated with this choice.

b. One-dimensional radiative–convective modeling

We model the atmosphere using NCAR’s Single Column Atmospheric Model (SCAM) (Hack et al. 2004). This model contains all of the physical parameterizations (including, e.g., those for aerosols, clouds, convection, and radiation) of CAM (Collins et al. 2004; McCaa et al. 2004), NCAR’s atmospheric general circulation model. We increase the model resolution to 100 vertical levels and decrease the time step to 150 s, compared to a default 26 levels and 1200 s used in SCAM. We set the top of the atmosphere incoming solar radiation to a constant 320 W m^{-2} , roughly 94% of the current global average, as appropriate for the Neoproterozoic. The surface temperatures the model produces at higher albedo values are roughly equivalent to those in the tropics in previous simulations of a Snowball in general circulation

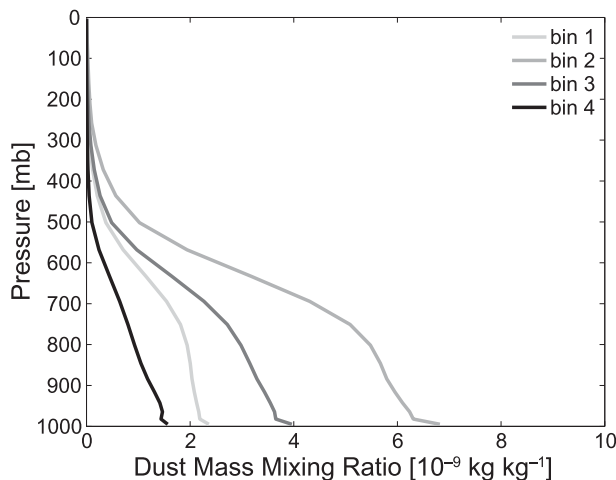


FIG. 2. Annual and tropical mean dust profile from the standard CAM aerosol dust climatology in each of the following four dust diameter bins: bin 1 (0.1–1.0 μm), bin 2 (1.0–2.5 μm), bin 3 (2.5–5.0 μm), and bin 4 (5.0–10.0 μm).

models (Pierrehumbert 2004, 2005). We average model results over 5 years of converged solutions.

We apply dust to the model by multiplying the tropical average of the seasonally varying standard CAM aerosol dust climatology by D (see section 2a) for each of the CAM dust size bins, which represent dust particles with diameter 0.1–1.0, 1.0–2.5, 2.5–5.0, and 5.0–10.0 μm . The standard dust profiles are shown in Fig. 2. Each dust bin has its own characteristic optical properties. Details of the dust aerosol parameterizations used in CAM and SCAM are provided in Collins et al. (2004). When the model was run with modern solar insolation (344 W m^{-2}) at a surface albedo of 0.15, the surface air temperature was 0.28°C cooler for $D = 1$ than for $D = 0$. This corresponds well with 0.20°C of dust-related surface cooling calculated by Mahowald et al. (2006b) with a three-dimensional dust model.

We set all other aerosols to zero except in simulations aimed at testing the sensitivity to other aerosol types (section 3c). Other than in simulations aimed at testing the sensitivity of our results to ozone concentrations (section 3c), we use the annual and zonal mean equatorial ozone profile from the standard CAM input files, which is based on Dutsch (1978).

We calculate the surface temperature from surface heat balance and assume a surface heat capacity equivalent to 10 m of water. This exact value does not affect our results since we drive the model with constant solar radiation. We calculate evaporation using the standard bulk aerodynamic formula, which would be appropriate over snow or ice, using a surface wind speed of 10 m s^{-1} .

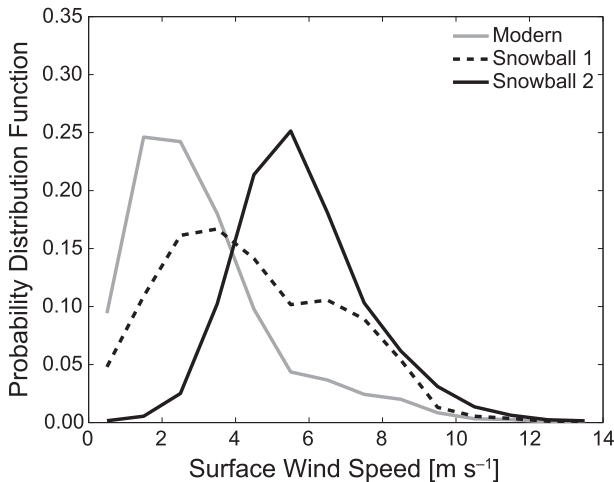


FIG. 3. PDF for surface wind speed over land in CAM. The three configurations are described in section 2a. Wind speeds are much higher in the two Snowball configurations.

3. Results

a. Dust concentrations

The CAM Snowball simulations described in section 2a yield surface wind speeds much higher than the Modern simulation, as demonstrated by the PDFs in Fig. 3. In combination with the dust fluxes generated for these velocities by the DEAD model (Fig. 1), Eq. (2) yield a total dust flux that is ~ 9 times higher in Snowball 1 than Modern and ~ 15 times higher in Snowball 2 ($S \sim 9\text{--}15$).

The CAM simulations also yield net snow accumulation over 45% of land regions in the Snowball 1 case and 70% in the Snowball 2 case. Since net snow accumulation would likely lead to glaciation this indicates that it is reasonable to choose a value for f_g between 0.45 and 0.7. In combination with our estimate for modern dust source region surface area (12.5%, section 2a), Eq. (3) then yields an increase factor in dust source region surface area between 2.5 and 4.5 ($A \sim 2.5\text{--}4.5$). We repeat, however, that it is difficult to estimate f_g . For example, A would be reduced if f_g were larger because of glacial flow, and our treatment neglects preferential dust mobilization from low-lying regions and the potential for additional dust production from net ablation zones. Based on these calculations and on the increased aerosol lifetime ($L \sim 1.5$, section 2a), we conclude that the atmospheric dust aerosol loading was likely one to two orders of magnitude higher than modern during Snowball episodes ($D \sim 30\text{--}100$), with the total dust burden increasing from a modern value of 39 Tg to a Snowball value of 1.3–3.9 Pg. Below we examine the effect on global climate of dust aerosol concentrations between 1 and 40 times present-day values.

b. Climate response

Consistent with previous results (Pierrehumbert 2004, 2005), increasing $p\text{CO}_2$ from 10^{-4} to 10^{-1} bar with dust aerosols at current levels raises the global average surface temperature by 17.9°C with a surface albedo of 0.5 and by only 13.0°C with a surface albedo of 0.7 (Fig. 4). Importantly, we find that increasing the dust loading causes a substantial surface warming, particularly at high values of the surface albedo and at relatively high $p\text{CO}_2$ (Fig. 4). For example, increasing dust by a factor of 40 in an atmosphere containing 0.1 bar of CO_2 causes 29.4°C warming for a surface albedo of 0.7, which is 2.3 times larger than the warming caused by a 1000-fold increase in $p\text{CO}_2$ at this surface albedo (Fig. 4).

For modern dust levels and a surface albedo of 0.8, an extremely cold state is possible (Fig. 4). The surface albedo is so high that an inversion forms, convection ceases entirely, there are very few clouds, and the cloud radiative forcing is reduced to zero, resulting in very low surface temperatures. This cold state exists for all values of $p\text{CO}_2$ examined ($10^{-4}\text{--}10^{-1}$ bar). For $p\text{CO}_2 > 10^{-4}$ bar, a warmer state similar to the lower albedo simulations is also possible at modern dust levels and a surface albedo of 0.8. This type of multiple equilibria in SCAM is similar to that described by Abbot and Tziperman (2009). Since this behavior occurs at an extremely high surface albedo and does not affect our main conclusions, though we consider it an interesting curiosity, we will discuss it no further.

c. Sensitivity analysis

In this section we describe tests of the sensitivity of our results to changes in the values of uncertain parameters. First we consider the optical properties of the dust aerosol and its vertical profile. The standard value of the single-scattering albedo (SSA) in the visible–near infrared (NIR) in SCAM and CAM, which adequately describes the optical properties of modern mineral dust, is ~ 0.95 . The mineralogical composition of dust strongly affects its optical properties; for example, high hematite content leads to decreased SSA (Sokolik and Toon 1999). The mineralogy of Neoproterozoic dust aerosol is not known and its optical properties are therefore uncertain. We carried out test simulations with the SSA in the visible and near infrared reduced by 10%, to ~ 0.86 , and by 20%, to ~ 0.76 . The increase in warming relative to the control provided by a 10% decrease in the dust SSA is $\sim 20^\circ\text{C}$ with a surface albedo of 0.6 and $\sim 30^\circ\text{C}$ with a surface albedo of 0.7 (Table 1). A 20% decrease in the SSA resulted in $\sim 30^\circ\text{C}$ and $\sim 40^\circ\text{C}$ of extra warming relative to the control with a surface albedo of 0.6 and 0.7, respectively. Although we do not argue for these values

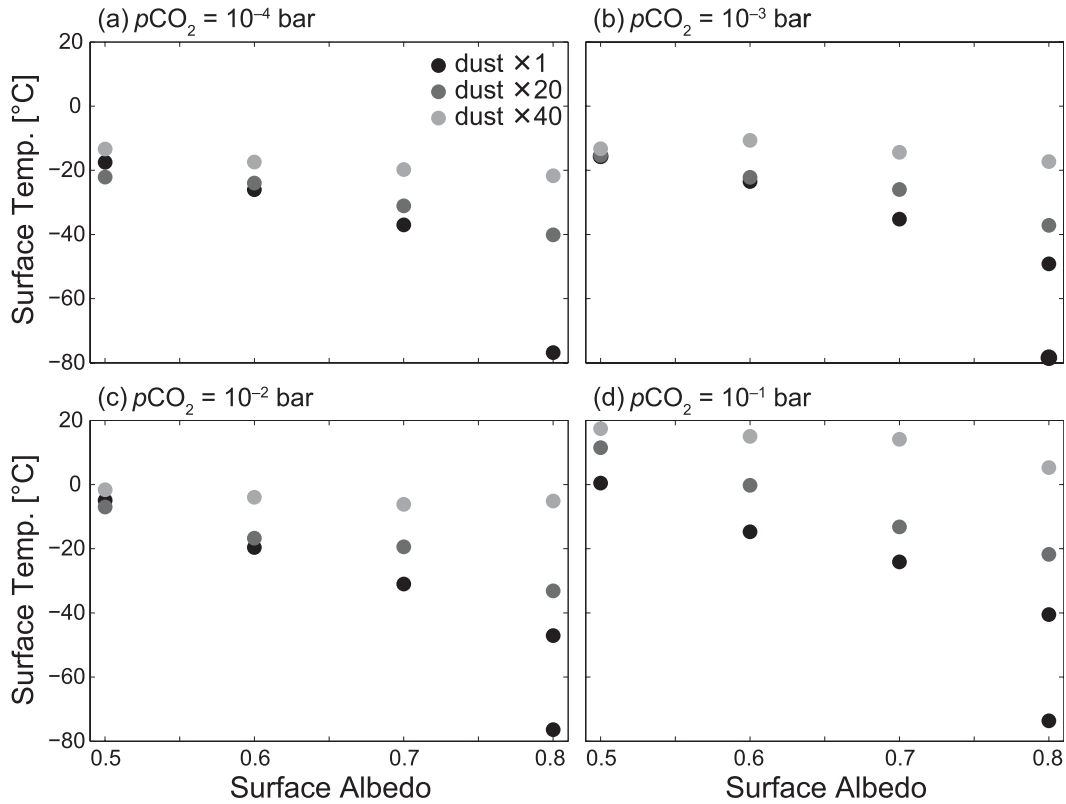


FIG. 4. Surface temperature as a function of the surface albedo, $p\text{CO}_2$, and dust loading. The dust profile is the modern tropical average, 20 times this at every vertical level, or 40 times this at every vertical level. In (b), (c), and (d) two points representing dust $\times 1$ at an albedo of 0.8 exist because of the existence of multiple climate equilibria under these conditions. See text for details.

of the SSA, this implies that our results from section 3b may represent conservative estimates for the radiative effects of a given dust loading.

The vertical distribution of dust aerosol during Snowball episodes may have differed from the modern. To test the effect of changes in the dust profile shape, we first fit the following equation to the modern dust profile in each size bin,

$$d(p) = d_0 \left[1 + \tanh\left(\frac{p - p_c}{\Delta p}\right) \right], \quad (4)$$

where $d(p)$ is the dust mass mixing ratio as a function of atmospheric pressure p , d_0 is chosen so that the total column dust loading in each size bin is not changed, and p_c and Δp are free parameters. Adopting the values $p_c = 650$ mb and $\Delta p = 200$ mb produces a reasonable fit to the modern dust profile (Fig. 5). We find that increasing p_c to 800 and 950 mb, which concentrates the dust at low levels, has only a minimal effect on the equilibrated climate (Table 1).

We now present sensitivity tests to a more broad set of parameters. For these calculations we set the vertical

and temporal resolution to the default values used in SCAM (26 vertical levels and 1200 s time steps). Halving the surface wind speed in SCAM to 5 m s^{-1} with fixed dust concentrations generally reduced surface turbulent fluxes of latent and sensible heat and so increased the surface temperature by about $2^\circ\text{--}3^\circ\text{C}$. However, given the demonstrated sensitivity of dust concentrations on the zonal wind velocity (Fig. 1), the sensitivity of the

TABLE 1. Surface temperature for $20\times$ modern dust as a function of surface albedo α and $p\text{CO}_2$ (bar) in the following cases: standard dust profile and optical properties (Control), dust aerosol single-scattering albedo in the visible and near infrared reduced by 10% (SSA 1), dust aerosol single-scattering albedo in the visible and near infrared reduced by 20% (SSA 2), p_c in Eq. (4) chosen to be 800 mb, and p_c in Eq. (4) chosen to be 950 mb.

	$\alpha = 0.6$		$\alpha = 0.7$	
$p\text{CO}_2$	0.01	0.1	0.01	0.1
Control	-11.9	1.1	-21.9	-12.4
SSA 1	9.7	23.1	0.9	20.7
SSA 2	18.3	37.4	10.9	33.1
Profile 1	-12.9	1.3	-21.4	-9.2
Profile 2	-8.1	1.4	-19.7	-6.2

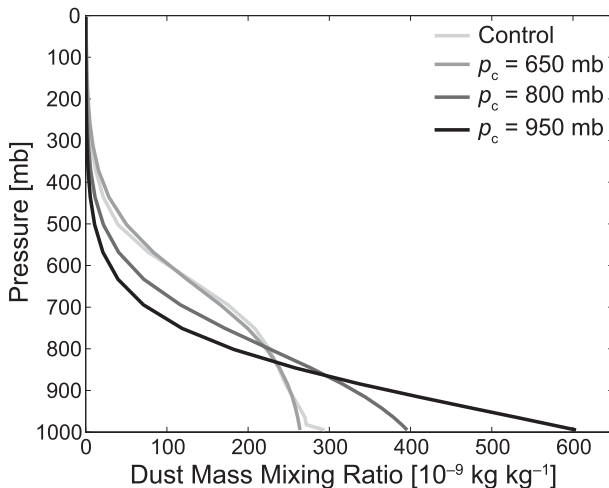


FIG. 5. Total (sum over all size bins) dust mass mixing ratio as a function of atmospheric pressure in the standard case (Control) and for different values of p_c in Eq. (4). In all cases $\Delta p = 200$ mb.

system to this parameter is probably much larger. We also performed calculations in which we coupled the SCAM atmosphere to the glacier land surface type from Community Land Model (CLM), NCAR's land surface model. The resulting surface albedo, produced by the calculated mixture of glacier surface and snow, was usually near 0.8 and the radiative–convective results similar to our higher-surface-albedo simulations.

Ozone concentrations are expected to be somewhat lower in the stratosphere of an oxygen-poor atmosphere (Segura et al. 2003), though the atmospheric chemistry under Snowball conditions may lengthen the lifetime of ozone. We therefore repeated the simulations with ozone concentrations 10 times lower and higher than modern. Decreasing the ozone concentration by a factor of 10 resulted in changes to the surface temperature of only a few degrees Celsius. When we increased the ozone concentration at each level by a factor of 10, the warming effect of adding dust was reduced by up to 50% because of increased solar absorption by ozone, but our qualitative results remained unchanged.

We found very little change in our results when we increased the concentration of sulfuric acid aerosols to 5 times the current tropical average, which might be appropriate as a long-term average concentration during a Snowball, given the more sluggish hydrological cycle and continued volcanic outgassing of SO_2 . Even when we increased the stratospheric volcanic aerosol concentration to 100 times its twentieth-century tropical average, an extreme value even following strong eruptions, we found only a slight cooling of a few degrees Celsius in all cases. In the even more unlikely case of stratospheric volcanic aerosol concentration 1000 times

its twentieth-century tropical average there was a dramatic cooling of $30^\circ\text{--}40^\circ\text{C}$ in all cases. This implies that, although volcanic ash could play a role in Snowball deglaciation by darkening the surface (Abbot and Pierrehumbert 2010), the aerosols resulting from extremely large eruptions would likely have a cooling effect during their lifetime in the atmosphere, though for reasonable posteruption aerosol concentrations this cooling would be small.

4. Discussion

The large increases in the lifetime and source of soil dust aerosols under the conditions expected during a Snowball event imply that atmospheric dust concentrations would have been higher than modern unless exposed continental area was less than 0.5%–1% of the total land area, which seems unlikely. As shown above, the additional dust can provide substantial positive radiative forcing above a highly reflective surface. Since we consider the planet from the relatively abstract perspective of a one-dimensional model forced by global and annual mean insolation, the qualitative response of the surface temperature to changes in soil dust concentrations (Fig. 4) is more important than the exact surface temperature values calculated by the model. For example, the fact that the surface temperature is 0.4°C with $p\text{CO}_2 = 10^{-1}$ bar, a surface albedo of 0.50 and modern dust levels should not be taken as a prediction that deglaciation would occur for these exact conditions. One can, nevertheless, take confidence in the result that for higher surface albedos the increase in dust aerosol concentrations that we expect to occur during a Snowball event can provide significantly more warming than large increases in $p\text{CO}_2$. As mentioned previously, it is estimated that $p\text{CO}_2$ was 0.01–0.08 bar during the glaciation ~ 635 million years ago (Bao et al. 2008, 2009). Although previous studies have shown that these levels of CO_2 might not be sufficient to deglaciate a Snowball, especially if thick sea ice developed, they could suffice if dust aerosol concentrations were somewhat higher than they are today.

We calculate S by integrating the wind speed-dependent dust lofting over the distribution of wind speeds expected during a Snowball [Eq. (2)]. However, it is possible that mechanical weathering rates, though enhanced, may not be rapid enough to sustain this value of S ($=9\text{--}15$) and may in effect limit the atmospheric dust loading. Modern dust production, calculated by dividing the dust loading in Mahowald et al. (2006b) by its lifetime, is $\sim 4200 \text{ Tg yr}^{-1}$. Dividing this value by the surface area of dust-producing regions ($\sim 12.5\%$, see section 2), yields an average flux of $\sim 0.22 \text{ kg m}^{-2} \text{ yr}^{-1}$, equivalent to

a denudation rate of 0.08 mm yr^{-1} for an assumed dust density of 2700 kg m^{-3} . Enhancing this by a factor of 9–15, as required by our calculations, implies a denudation rate of $0.7\text{--}1.2 \text{ mm yr}^{-1}$. A potential analog for exposed, low-latitude continental area during a Snowball is the semiarid Tibetan Plateau, where winter land surface temperatures are $\sim 0^\circ\text{C}$ during the day and plummet to approximately -30°C at night (Oku et al. 2006). The diurnal variation land surface temperature is somewhat smaller during summer, but still large ($\sim 5^\circ$ to $\sim 25^\circ\text{C}$). Though the summer temperatures are much higher than expected for dust-producing regions during a Snowball, it is arguably the large diurnal variations in temperature, rather than the absolute values, that lead to increased physical weathering rates due to thermal expansion and contraction of the rocks. The average denudation rate of the Tibetan Plateau is $\sim 2.3 \text{ mm yr}^{-1}$ or about 29 times greater than the average of dust-producing regions. Therefore, we find that an enhancement in dust production by a factor of 9–15 is reasonable in exposed low-latitude continental area during a Snowball, where comparable diurnal temperature variations are expected to exist year-round.

Two prominent features of our results merit further discussion. First, with increasing surface albedo the surface temperature becomes less sensitive to changes in $p\text{CO}_2$ but much more sensitive to changes in dust concentrations (Fig. 4). The reason for the former is that, at low values of the surface albedo, the surface absorbs more solar radiation and emits more infrared radiation. Increasing $p\text{CO}_2$, which absorbs and reemits infrared radiation, leads to more warming. Additionally, water vapor and cloud feedbacks are stronger at higher temperatures, contributing to the increased sensitivity of the low-albedo cases to changes in $p\text{CO}_2$. The higher sensitivity to changes in dust concentrations at high values of the surface albedo is partly because the negative radiative forcing due to upward scattering of solar radiation by increased dust is less important over a glaciated surface, which is already highly reflective. Additionally, absorption by dust is increased when the surface albedo is high because shortwave radiation is reflected from the icy surface and has a much longer pathlength in the atmosphere.

A second feature is that the radiative forcing by dust aerosols is noticeably smaller at low $p\text{CO}_2$ (Fig. 4). This is because at low $p\text{CO}_2$, with dust aerosol concentrations comparable to or only slightly higher than modern and a high surface albedo, a temperature inversion develops in the lower troposphere. The inversion develops because infrared cooling by CO_2 is not strong enough to compensate for heating due to absorption of shortwave radiation by the dust. As a result, the dusty regions of the troposphere heat up, stabilize the troposphere against

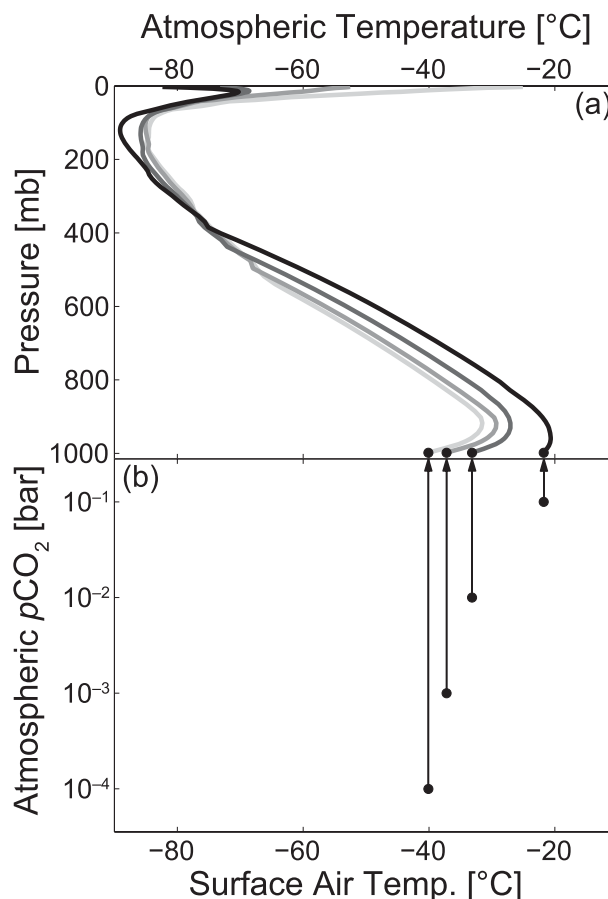


FIG. 6. Decrease in the atmospheric temperature inversion and rapid surface air temperature increase as $p\text{CO}_2$ is increased. (a) Vertical profiles of atmospheric temperature and (b) surface air temperature at different $p\text{CO}_2$. In all cases the surface albedo is 0.8 and dust aerosol loading is increased by a factor of 20. Lines of successively darker color in (a) represent increased $p\text{CO}_2$, as shown in (b).

convective mixing, and limit the surface warming effect of dust. As $p\text{CO}_2$ is increased, the atmosphere cools and the surface warms until the destabilizing influence is sufficient to cause convection and break the inversion (Figs. 6 and 7). When this occurs, shortwave heating by the dust is mixed into the entire troposphere, causing the surface temperature to increase dramatically and suddenly.

Although a global-scale temperature inversion would represent an extreme climatic event, it is not implausible. The atmospheric temperature profile on Mars, for example, can remain inverted for months at a time during global dust storms (Gurwell et al. 2005). Additionally, the fact that a one-dimensional radiative–convective model produces a temperature inversion under certain conditions does not mean that the entire planet would be subject to one in these cases. Consider, for example, the ozone layer, which produces a uniform stratospheric

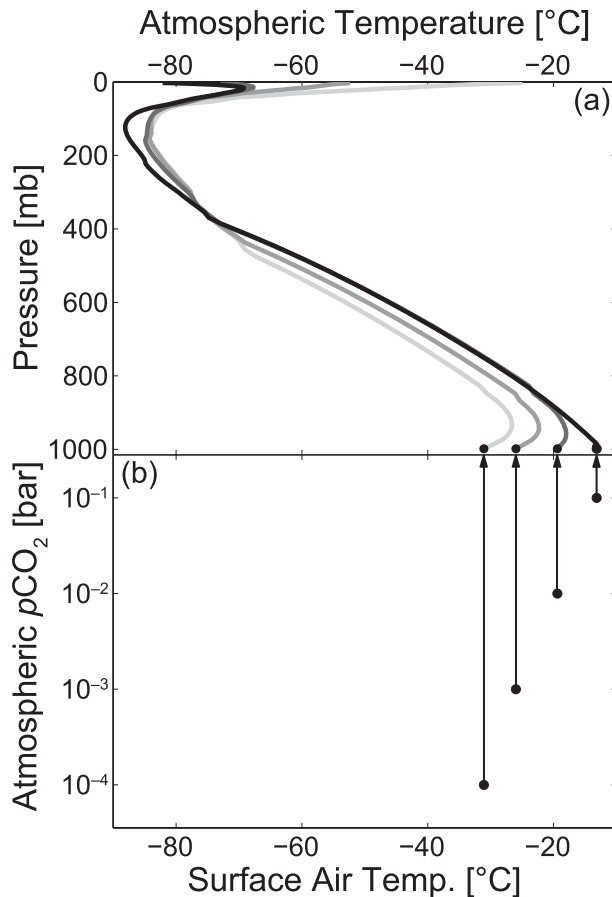


FIG. 7. As in Fig. 6, but with a surface albedo of 0.7.

temperature inversion in one-dimensional radiative–convective models despite significant heterogeneity in the actual ozone stratospheric inversion. It is likely that a dust-induced inversion would only prevail during a Snowball over regions covered with high-albedo snow and ice, whereas the atmosphere would be convecting over low-albedo continental regions. This is important because convection over such dust source regions would loft the dust that would allow the inversion to persist elsewhere. Resolving these issues requires three-dimensional dust–climate modeling. However, we feel that our one-dimensional results provide useful insight into the issues affecting atmospheric stability under Snowball conditions.

The fact that high dust levels only cause strong warming once $p\text{CO}_2$ is high enough to destroy the inversion caused by shortwave absorption by dust (Figs. 4, 6 and 7) has two important implications for the evolution of surface temperature over the lifetime of a global glaciation. First, even though dust aerosols would play an important role in global radiative balance during a Snowball event and could allow deglaciation, CO_2 outgassing would

still control the duration of a Snowball. At current CO_2 outgassing rates, it would take only 0.2–2 million years to increase the $p\text{CO}_2$ to 0.01–0.1 bar, but the lifetime of a Snowball could be extended if small openings in the sea ice allowed air–sea gas exchange and some of the outgassed CO_2 were taken up by dissolution of carbonate sediments (Higgins and Schrag 2003) or by seafloor weathering and carbonatization (Le Hir et al. 2008). A second implication is that the deglaciation is expected to be abrupt. A young Snowball would quickly develop a dusty atmosphere with an inversion in its vertical temperature profile. As $p\text{CO}_2$ increased because of continued volcanic outgassing, relatively little surface warming would occur until the inversion were broken, at which time the surface temperature would quite suddenly exceed freezing.

The CAM radiation code does not include the longwave radiative effects of dust aerosol. These effects are small, but nonzero, in the modern climate and could be even more important in a climate with less water vapor, fewer clouds, and much more dust (Miller and Tegen 1998; Yoshioka et al. 2007). Including the longwave radiative effects of dust would increase the estimates of warming induced by dust during a Snowball, which means that our calculations probably underestimate the warming that would be produced by a particular dust aerosol loading. If the dust longwave radiative forcing is large enough, however, it might disrupt the low- CO_2 inversions that we found in our calculations. Resolving this issue requires calculations that include the longwave radiative effects of dust aerosol.

5. Conclusions

We have shown that very reasonable increases in dust aerosol concentrations during a Snowball cause significant surface warming when $p\text{CO}_2$ is above a few hundredths of a bar. This effect increases with increasing surface albedo, partially compensating for the greater fraction of sunlight reflected by the bright surface. This substantial effect on surface temperature may be sufficient to allow deglaciation of a Snowball, which has heretofore been difficult to produce in global climate models that did not include the effect of dust aerosols on the atmospheric energy budget. The deglaciation would occur suddenly and only once $p\text{CO}_2$ reached a threshold value (a few hundredths of a bar) required for convective mixing of the warming caused by the dust into the lower troposphere. This fits nicely with recent work, which has shown that dust accumulation could lower the surface albedo in net ablating regions enough to lead to deglaciation (Abbot and Pierrehumbert 2010). We conclude that dust effects, which have previously been

neglected in climate simulations, can allow a Snowball to deglaciate. More confidence in these results would come from GCM simulations that include dust.

Acknowledgments. We thank J. Higgins, P. Hoffman, D. Schrag, and C. Zender for comments and advice. We thank Stephen Warren and two anonymous reviewers for helping to improve this manuscript. This work was funded by the NSF paleoclimate program (ATM-0455470), the NSF P2C2 program (ATM-0902844), and the Canadian Institute for Advanced Research. I.H. was funded by a Harvard University Origins of Life Initiative Graduate Fellowship.

REFERENCES

- Abbot, D. S., and E. Tziperman, 2009: Controls on the activation and strength of a high-latitude convective cloud feedback. *J. Atmos. Sci.*, **66**, 519–529.
- , and R. T. Pierrehumbert, 2010: Mudball: Surface dust and Snowball Earth deglaciation. *J. Geophys. Res.*, **115**, D03104, doi:10.1029/2009JD012007.
- , M. Huber, G. Bousquet, and C. C. Walker, 2009: High-CO₂ cloud radiative forcing feedback over both land and ocean in a global climate model. *Geophys. Res. Lett.*, **36**, L05702, doi:10.1029/2008GL036703.
- Allen, P. A., and J. I. Etienne, 2008: Sedimentary challenge to Snowball Earth. *Nat. Geosci.*, **1**, 817–825.
- Bao, H. M., J. R. Lyons, and C. M. Zhou, 2008: Triple oxygen isotope evidence for elevated CO₂ levels after a Neoproterozoic glaciation. *Nature*, **453**, 504–506.
- , I. J. Fairchild, P. M. Wynn, and C. Spötl, 2009: Stretching the envelope of past surface environments: Neoproterozoic glacial lakes from Svalbard. *Science*, **323**, 119–112.
- Bierwirth, E., and Coauthors, 2009: Spectral surface albedo over Morocco and its impact on radiative forcing of Saharan dust. *Tellus*, **61B**, 252–269.
- Bonan, G. B., S. Levis, L. Kergoat, and K. W. Oleson, 2002: Landscapes as patches of plant functional types: An integrating concept for climate and ecosystem models. *Global Biogeochem. Cycles*, **16**, 1021, doi:10.1029/2000GB001360.
- Caldeira, K., and J. F. Kasting, 1992: Susceptibility of the early Earth to irreversible glaciation caused by carbon-dioxide clouds. *Nature*, **359**, 226–228.
- Collins, W. D., and Coauthors, 2004: Description of the NCAR Community Atmosphere Model (CAM 3.0). NCAR Tech. Note, NCAR/TN-464+STR, 214 pp.
- Donnadieu, Y., F. Fluteau, G. Ramstein, C. Ritz, and J. Besse, 2003: Is there a conflict between the Neoproterozoic glacial deposits and the Snowball Earth interpretation: An improved understanding with numerical modeling. *Earth Planet. Sci. Lett.*, **208**, 101–112.
- Dutsch, H. U., 1978: Vertical ozone distribution on a global scale. *Pure Appl. Geophys.*, **116**, 511–529.
- Elliott, C., 2008: Influence of temperature and moisture availability on physical rock weathering along the Victoria Land coast, Antarctica. *Antarct. Sci.*, **20**, 61–67.
- Evans, D. A. D., 2000: Stratigraphic, geochronological, and paleomagnetic constraints upon the Neoproterozoic climatic paradox. *Amer. J. Sci.*, **300**, 347–433.
- Gurwell, M. A., E. A. Bergin, G. J. Melnick, and V. Tolls, 2005: Mars surface and atmospheric temperature during the 2001 global dust storm. *Icarus*, **175**, 23–31.
- Hack, J. J., J. E. Truesdale, J. A. Pedretti, and J. C. Petch, cited 2004: SCAM user's guide. [Available online at <http://www.cesm.ucar.edu/models/atm-cam/docs/scam/>]
- Halevy, I., R. T. Pierrehumbert, and D. P. Schrag, 2009: Radiative transfer in CO₂-rich paleoatmospheres. *J. Geophys. Res.*, **114**, D18112, doi:10.1029/2009JD011915.
- Hall, K., 1998: Rock temperatures and implications for cold region weathering. II: New data from Rothera, Adelaide Island, Antarctica. *Permafrost Periglacial Processes*, **9**, 47–55.
- Harrison, S. P., K. E. Kohfeld, C. Roelandt, and T. Claquin, 2001: The role of dust in climate changes today, at the Last Glacial Maximum and in the future. *Earth Sci. Rev.*, **54**, 43–80.
- Held, I. M., and B. J. Soden, 2006: Robust responses of the hydrological cycle to global warming. *J. Climate*, **19**, 5686–5699.
- Higgins, J. A., and D. P. Schrag, 2003: Aftermath of a Snowball Earth. *Geochem. Geophys. Geosyst.*, **4**, 1028, doi:10.1029/2002GC000403.
- Hoffman, P. F., and Z.-X. Li, 2009: A palaeogeographic context for Neoproterozoic glaciation. *Palaeogeogr. Palaeoclimatol. Palaeoecol.*, **277**, 158–172.
- , A. J. Kaufman, G. P. Halverson, and D. P. Schrag, 1998: A Neoproterozoic Snowball Earth. *Science*, **281**, 1342–1346.
- , J. W. Crowley, D. T. Johnston, D. S. Jones, and D. P. Schrag, 2008: Snowball prevention questioned. *Nature*, **456**, E7, doi:10.1038/nature07655.
- Hyde, W. T., T. J. Crowley, S. K. Baum, and W. R. Peltier, 2000: Neoproterozoic 'Snowball Earth' simulations with a coupled climate/ice-sheet model. *Nature*, **405**, 425–429.
- Kerr, R. A., 2000: An appealing Snowball Earth that's still hard to swallow. *Science*, **287**, 1734–1736.
- Kirschvink, J., 1992: Late Proterozoic low-latitude global glaciation: The Snowball Earth. *The Proterozoic Biosphere: A Multidisciplinary Study*, J. Schopf and C. Klein, Eds., Cambridge University Press, 51–52.
- Konishchev, V. N., 1982: Characteristics of cryogenic weathering in the permafrost zone of the European USSR. *Arct. Alp. Res.*, **14**, 261–265.
- Krinner, G., O. Boucher, and Y. Balkanski, 2006: Ice-free glacial northern Asia due to dust deposition on snow. *Climate Dyn.*, **27**, 613–625.
- Le Hir, G., G. Ramstein, Y. Donnadieu, and R. T. Pierrehumbert, 2007: Investigating plausible mechanisms to trigger a deglaciation from a hard Snowball Earth. *C. R. Geosci.*, **339**, 274–287.
- , —, —, and Y. Godderis, 2008: Scenario for the evolution of atmospheric pCO₂ during a Snowball Earth. *Geology*, **36**, 47–50.
- Mahowald, N. M., D. R. Muhs, S. Levis, P. J. Rasch, M. Yoshioka, C. S. Zender, and C. Luo, 2006a: Change in atmospheric mineral aerosols in response to climate: Last Glacial period, preindustrial, modern, and doubled carbon dioxide climates. *J. Geophys. Res.*, **111**, D10202, doi:10.1029/2005JD006653.
- , M. Yoshioka, W. D. Collins, A. J. Conley, D. W. Fillmore, and D. B. Coleman, 2006b: Climate response and radiative forcing from mineral aerosols during the Last Glacial Maximum, pre-industrial, current and doubled-carbon dioxide climates. *Geophys. Res. Lett.*, **33**, L20705, doi:10.1029/2006GL026126.
- McCaa, J., M. Rothstein, B. Eaton, J. Rosinski, E. Kluzek, and M. Vertenstein, cited 2004: User's guide to the NCAR Community Atmosphere Model (CAM 3.0). [Available

- online at <http://www.cesm.ucar.edu/models/atm-cam/docs/usersguide/>]
- Miller, R. L., and I. Tegen, 1998: Climate response to soil dust aerosols. *J. Climate*, **11**, 3247–3267.
- Oku, Y., I. Hirohiko, S. Haginoya, and Y. Ma, 2006: Recent trends in land surface temperature on the Tibetan Plateau. *J. Climate*, **19**, 2995–3003.
- Peltier, W. R., and Y. G. Liu, 2008: Carbon cycling and Snowball Earth. Reply. *Nature*, **456**, E9–E10, doi:10.1038/nature07656.
- , —, and J. W. Crowley, 2007: Snowball Earth prevention by dissolved organic carbon remineralization. *Nature*, **450**, 813–818.
- Pierrehumbert, R. T., 2002: The hydrologic cycle in deep-time climate problems. *Nature*, **419**, 191–198.
- , 2004: High levels of atmospheric carbon dioxide necessary for the termination of global glaciation. *Nature*, **429**, 646–649.
- , 2005: Climate dynamics of a hard Snowball Earth. *J. Geophys. Res.*, **110**, D011111, doi:10.1029/2004JD005162.
- Pollard, D., and J. F. Kasting, 2005: Snowball Earth: A thin-ice solution with flowing sea glaciers. *J. Geophys. Res.*, **110**, C07010, doi:10.1029/2004JC002525.
- , and —, 2006: Reply to comment by Stephen G. Warren and Richard E. Brandt on “Snowball Earth: A thin-ice solution with flowing sea glaciers.” *J. Geophys. Res.*, **111**, C09017, doi:10.1029/2006JC003488.
- Segura, A., K. Krellove, J. F. Kasting, D. Sommerlatt, V. Meadows, D. Crisp, M. Cohen, and E. Mlawer, 2003: Ozone concentrations and ultraviolet fluxes on Earth-like planets around other stars. *Astrobiology*, **3**, 689–708.
- Sokolik, I. N., and O. B. Toon, 1999: Incorporation of mineralogical composition into models of the radiative properties of mineral aerosol from UV to IR wavelengths. *J. Geophys. Res.*, **104** (D8), 9423–9444.
- Tetzlaff, G., 1983: Albedo of the Sahara. *Satellite Measurement of Radiation Budget Parameters*, E. Raschke et al., Eds., 60–63.
- Trindade, R. I. F., and M. Macouin, 2007: Palaeolatitude of glacial deposits and palaeogeography of Neoproterozoic ice ages. *C. R. Geosci.*, **339**, 200–211.
- Warren, S. G., and R. E. Brandt, 2006: Comment on “Snowball Earth: A thin-ice solution with flowing sea glaciers” by David Pollard and James F. Kasting. *J. Geophys. Res.*, **111**, C09016, doi:10.1029/2005JC003411.
- , —, T. C. Grenfell, and C. P. McKay, 2002: Snowball Earth: Ice thickness on the tropical ocean. *J. Geophys. Res.*, **107**, 3167, doi:10.1029/2001JC001123.
- Weaver, C. J., P. Ginoux, N. C. Hsu, M. D. Chou, and J. Joiner, 2002: Radiative forcing of Saharan dust: GOCART model simulations compared with ERBE data. *J. Atmos. Sci.*, **59**, 736–747.
- Yoshioka, M., N. M. Mahowald, A. J. Conley, W. D. Collins, D. W. Fillmore, C. S. Zender, and D. B. Coleman, 2007: Impact of desert dust radiative forcing on Sahel precipitation: Relative importance of dust compared to sea surface temperature variations, vegetation changes, and greenhouse gas warming. *J. Climate*, **20**, 1445–1467.
- Zender, C. S., H. S. Bian, and D. Newman, 2003: Mineral Dust Entrainment and Deposition (DEAD) model: Description and 1990s dust climatology. *J. Geophys. Res.*, **108**, 4416, doi:10.1029/2002JD002775.